

PAPER • OPEN ACCESS

## Derivation of the Hubble parameter using galaxy clusters

To cite this article: A Kozmanyán *et al* 2017 *J. Phys.: Conf. Ser.* **841** 012004

View the [article online](#) for updates and enhancements.

### Related content

- [THE HUBBLE PARAMETER REVISITED](#)  
Sidney van den Bergh
- [THE HUBBLE PARAMETER](#)  
Sidney van den Bergh
- [COLLISIONS AND RELAXATION IN GALAXY CLUSTERS.](#)  
P. D. Noerdlinger



**IOP | ebooks™**

Bringing you innovative digital publishing with leading voices to create your essential collection of books in STEM research.

Start exploring the collection - download the first chapter of every title for free.

# Derivation of the Hubble parameter using galaxy clusters

**A Kozmanyán<sup>1</sup>, H Bourdin<sup>1</sup>, G de Gasperis<sup>1,2</sup>, P Mazzotta<sup>1,3</sup> and N Vittorio<sup>1,2</sup>**

<sup>1</sup>Dipartimento di Fisica, Università di Roma “Tor Vergata”, via della Ricerca Scientifica 1, I-00133, Roma, Italy

<sup>2</sup>Sezione INFN Roma 2, via della Ricerca Scientifica 1, I-00133, Roma, Italy

<sup>3</sup>Harvard Smithsonian Centre for Astrophysics, 60 Garden Street, Cambridge, MA 02138, USA

E-mail: [arpine.kozmanyán@roma2.infn.it](mailto:arpine.kozmanyán@roma2.infn.it)

**Abstract.** In this work we describe a possible way to use X-ray and microwave observations of nearby galaxy clusters to derive the value of the Hubble constant, that parametrises the expansion rate of the Universe. We provide a brief introduction to the Sunyaev-Zel’dovich effect that allows to detect galaxy clusters at microwave frequencies, and the method to combine it with X-ray observables. We emphasize what kind of considerations should be done when applying the method on real data and study the effect of the geometry of the clusters on the final result.

## 1. Introduction

Galaxy clusters are the largest gravitationally collapsed structures known in the Universe. They are dominated by dark matter, but also contain a considerable amount of hot ionised gas called Intra-Cluster Medium (ICM). This ionised medium allows the detection of galaxy clusters in at least two ways. The ICM electrons emit bremsstrahlung radiation at X-ray wavelengths. Additionally, when passing through a galaxy cluster the Cosmic Microwave Background (CMB) Radiation photons undergo Inverse Compton scattering by the ICM electrons. This introduces a modification to the original blackbody spectrum of the CMB radiation (the so called Sunyaev-Zel’dovich effect), thus making it possible to detect the clusters using the CMB as a backlight.

The two effects are interconnected, since they both depend on the distribution of the ICM electrons in the galaxy cluster. Using both of the signals a thorough investigation of matter distribution in the cluster can be done. The knowledge of the distribution of matter inside the cluster on the other hand allows to model the expected Sunyaev-Zel’dovich (SZ) and X-ray signals for a given cluster assuming a certain cosmological model. A derivation of the best-fitting parameter values can then be done comparing the modeled signals with the observed ones.

The physics of the ICM is quite complicated and our knowledge of it is limited, however, galaxy clusters could provide a complementary cosmological probe along with the classical ones such as type Ia supernovae, CMB, or baryon acoustic oscillations. The quantity that can be constrained using SZ and X-ray signals jointly is the angular diameter distance for individual clusters. Hence cosmological parameters such as the Hubble constant today, the total density of matter and the equation of state of dark energy can be potentially constrained.



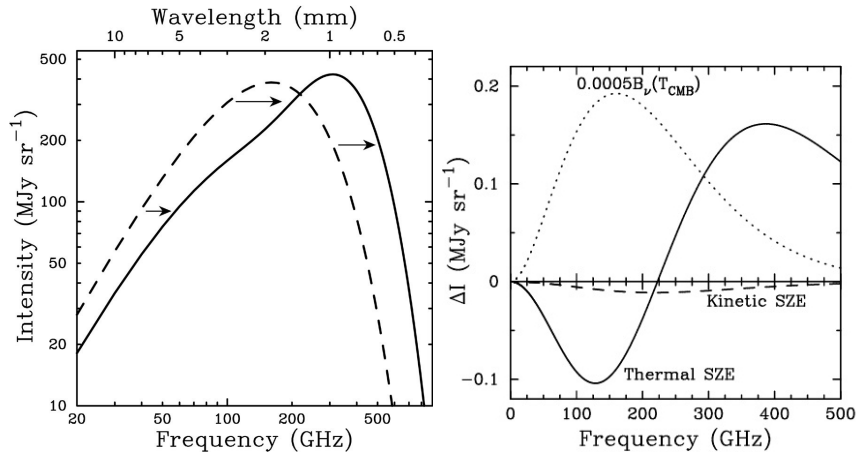


**Figure 1.** Left: The distortion of the blackbody CMB power spectrum (dashed line) due to the SZ effect (solid line). The amplitude of the effect is exaggerated in order to show visually the overall shift of the spectrum to higher energies. Right: The amplitude of the distortion depending on frequency for the thermal and kinematic effects. Both figures are taken from Carlstrom et al. [8].

At the moment, however, the data are not sensitive enough to be sensitive to the latter quantities. Instead, the Hubble constant can be estimated easily. Current estimates of the parameter from CMB anisotropies by the Planck Collaboration [1]  $H_0 = 66.93 \pm 0.62 \text{ km s}^{-1} \text{ Mpc}^{-1}$  seem to be in slight tension with the value derived by Riess et al. [2] using Cepheid-calibrated type Ia supernovae  $H_0 = 73.24 \pm 1.74 \text{ km s}^{-1} \text{ Mpc}^{-1}$ . Other probes such as the baryon acoustic oscillations provide recent results of  $H_0 = 68.0 \pm 1.1 \text{ km s}^{-1} \text{ Mpc}^{-1}$  by Cheng et al. [3] or in combination with CMB measurements from WMAP  $H_0 = 69.6 \pm 0.7 \text{ km s}^{-1} \text{ Mpc}^{-1}$  from Bennett et al. [4]. Using galaxy clusters, instead, Bonamente et al. [5] found a value of  $H_0 = 76.9_{-3.4-8.0}^{+3.9+10.0} \text{ km s}^{-1} \text{ Mpc}^{-1}$  for fixed  $\Omega_m = 0.3$  and  $\Omega_\Lambda = 0.7$  using a sample of 38 clusters. The newly available Planck data will allow to improve the estimate derived from galaxy clusters.

Our work is structured in the following way. We start with a brief introduction to the Sunyaev-Zel'dovich effect and its characteristics in Section 2. In the same section we give a short description of the methods of observation of the SZ signal from galaxy clusters at microwave frequencies (Section 2.1). In Section 3 we describe the method to derive the Hubble parameter and discuss our preliminary results about the systematics introduced by the geometry of the clusters. Finally, we summarise our conclusions in Section 4.

## 2. The Sunyaev Zel'dovich effect from Galaxy Clusters

Density perturbations in the primordial Universe get amplified due to gravity. Eventually they collapse under their own mass and form smaller structures that, after series of mergers, will combine into larger structures. In this way, by a hierarchical sequence of mergers of galaxies, the largest gravitationally bound structures such as clusters of galaxies are formed. The main constituent of the galaxy clusters is the dark matter ( $10^{13} - 10^{15} M_\odot$ ), which generates the gravitational potential felt by the luminous components. The latter are the hot ionised gas that constitutes the intra-cluster medium ( $10^{12} - 10^{14} M_\odot$ ) and the galaxies themselves ( $10^{11} - 10^{13} M_\odot$ ).

The variety of these components provides us with a number of ways to detect galaxy clusters. One can look at the light emitted by the stars in the member galaxies of the cluster at optical

and radio wavelengths. The electrons in the ICM also emit bremsstrahlung radiation that is possible to detect at X-ray wavelengths [6]. And finally the same electrons can Inverse Compton scatter part of the CMB photons that pass through the cluster on their way to us. This shifts the energies of the scattered photons to higher frequencies [7]. As a result, the original blackbody spectrum of the CMB gets distorted (see Fig. 1).

The exact shape of the distortion depends on the nature of the scattering between the photons and the electrons. In particular, we are interested in the scattering due to the thermal motion of the ICM electrons (thermal SZ), since it provides a way to detect the galaxy clusters using the CMB as a backlight.

Since in galaxy clusters the electron temperatures are very high ( $k_B T \simeq keV$ ), after the electron-photon scattering, the photons gain energy. As the Compton scattering conserves the photon number, the overall effect is a shift to higher energy of the initial Planck spectrum (illustrated in the left part of Fig. 1). As a result the measured CMB intensity is lower at frequencies  $\nu < \bar{\nu}$  and higher at frequencies above it as shown in the right part of Fig. 1. The frequency  $\bar{\nu}$  is where there is no variation in the intensity and it corresponds to  $\bar{\nu} = 217$  GHz for non-relativistic thermal SZ effect. This spectral signature can be used to identify galaxy clusters in the microwaves. The relative change in the CMB intensity introduced by the thermal SZ effect is:

$$\frac{\Delta I}{I_{CMB}} = g(x) \int \sigma_T n_e \frac{k_B T_e}{m_e c^2} dl. \quad (1)$$

Here  $g(x)$  is a function of dimensionless frequency  $x \equiv h\nu/k_B T_{CMB}$ ,  $I_{CMB}$  the CMB intensity,  $T_e$  the temperature of the ICM electrons,  $n_e$  the number density of the electrons and  $\sigma_T$ ,  $m_e$ ,  $c$  are the Thomson scattering cross-section, the electron mass and the speed of light respectively. Finally, the integration on  $dl$  is done along our line of sight. The function  $g(x)$  describes the spectral shape of the effect and has the following form:

$$g(x) = \frac{x^4 e^x}{(e^x - 1)^2} \left( x \frac{e^x + 1}{e^x - 1} - 4 \right). \quad (2)$$

The integral on the right-hand side of Eq. 1 is the Comptonisation parameter  $y$ :

$$y = \frac{\sigma_T}{m_e c^2} \int n_e \times k_B T_e \times dl = \frac{\sigma_T}{m_e c^2} \int P_e \times dl, \quad (3)$$

where we introduced the electron pressure profile as the product of the number density and the temperature ( $P_e = n_e \times k_B T_e$ ). The Comptonisation parameter  $y$  is the quantity that describes the amplitude of the SZ effect and depends on the cluster properties, i.e. the thermal electron pressure of the ICM along the line of sight.

Eq. 1 has been derived in the non-relativistic approximation for clusters of temperatures  $k_B T < 10 keV$ . At higher temperatures corrections need to be introduced to the above formulae that will eventually also shift the location of the characteristic frequency  $\bar{\nu}$  [9, 10].

An additional effect can be caused due to the overall peculiar motion of the galaxy cluster relative to the CMB rest frame (kinematic SZ effect). In this work we will concentrate only on the thermal effect and will denote it simply as SZ.

### 2.1. Observations of the thermal SZ signal from galaxy clusters

There is a large number of astrophysical and cosmological components that emit at microwave frequencies. Examples are the synchrotron emission generated by the relativistic cosmic-ray electrons spiraling in the Galactic magnetic field, the free-free emission that is the bremsstrahlung radiation from electron-ion collisions in our Galaxy, the thermal emission from dust grains on the Galactic plane and of course the CMB. The signal that we measure from

the sky is the sum of the contributions from all these components. In order to perform any physical investigation we need first to perform a component separation. This can be achieved by multifrequency observations making use of the different spectral signatures of the components [11, 12].

For illustration purposes let us assume to have only three components: the CMB with the SZ component embedded in it and the thermal emission from Galactic dust. The total signal at a given frequency and direction in the sky (the latter is characterised by a given pixel  $\vec{p}$  in the eventual map of the sky) can be written as the linear combination of the three components:

$$s(\vec{p}, \nu) = A_{CMB}(\vec{p}) + A_{SZ}(\vec{p}) * f_{SZ}(\nu) + A_{dust}(\vec{p}) * f_{dust}(\nu). \quad (4)$$

Here  $A_i(\vec{p})$  are the amplitudes of the component signals at a given direction  $\vec{p}$ , and  $f_i(\nu)$  are their spectral dependences. Note that  $A_i(\vec{p})$  depend only on the direction on the sky and  $f_i(\nu)$  instead depend only on the frequency and are defined by the model for the spectral dependence assumed for each component. In particular  $f_{SZ}(\nu)$  would be described by Eq. 2 and the thermal dust contribution can be described by a variety of gray-body spectra [12, 13]. The total signal  $s(\vec{p}, \nu)$  is a function of frequency and direction in the sky. Thus, having measurements of the total signal for a given pixel at different frequencies, one can solve a set of equations for a given pixel and derive the values for  $A_i(\vec{p})$ .

### 3. Derivation of the angular diameter distance from joint SZ and X-ray data of galaxy clusters

Both SZ signal and X-ray emission from galaxy clusters are caused by the ICM electrons. The SZ signal is the line-of-sight integral of the electron pressure as shown in Eq. 3. The X-ray surface brightness emission instead is the line-of-sight integral of the electron number density squared:

$$S_X \propto \int n_e^2 dl. \quad (5)$$

This means both of the signals depend on the physical size of the cluster along the line of sight.

When we observe the cluster we measure only its angular size and the redshift. However, the real physical size of the cluster given its angular size and redshift depends on the cosmological model. The relationship between the physical size of an object and its apparent angular size is given by a quantity called angular diameter distance:

$$D_A = \frac{l}{\theta}, \quad (6)$$

where  $l$  is the physical size of the object in Mpc and  $\theta$  is the corresponding angular size in radians. This quantity, on the other hand, depends on the cosmology of the Universe:

$$D_A = \frac{1}{1+z} \frac{c}{H_0} \times \begin{cases} \frac{1}{\sqrt{\Omega_k}} \sinh \left( \sqrt{\Omega_k} \int_0^z \frac{dz'}{E(z')} \right), & \text{for } \Omega_k > 0 \\ \int_0^z \frac{dz'}{E(z')}, & \text{for } \Omega_k = 0 \\ \frac{1}{\sqrt{|\Omega_k|}} \sin \left( \sqrt{|\Omega_k|} \int_0^z \frac{dz'}{E(z')} \right), & \text{for } \Omega_k < 0 \end{cases} \quad (7)$$

Here  $H_0$  is the value of the Hubble constant,  $c$  is the speed of light in vacuum and  $z$  the redshift of the object. The parameter  $\Omega_k = 1 - \Omega_m - \Omega_\Lambda$  is the curvature density of the Universe,  $\Omega_m$  the total density of matter and  $\Omega_\Lambda$  is the dark energy density. Finally, the factor  $E(z)$  is defined as  $E(z) = \sqrt{\Omega_m(1+z)^3 + \Omega_k(1+z)^2 + \Omega_\Lambda}$ . The three cases in Eq. 7 represent the cases with the Universe being negatively curved, flat and positively curved, respectively.

The relationship in Eq. 7 can be much simplified when dealing with objects at low redshift ( $z < 0.1$ ). It can be reduced to:

$$D_A \propto \frac{1}{H_0} \times z. \quad (8)$$

Then the SZ and X-ray signals from a cluster at a given redshift and with a given angular size depend on the value of  $H_0$ . Consequently the two signals would depend on different combinations of  $n_e$  and  $H_0$ :  $y \propto n_e H_0^{-1}$  and  $S_X \propto n_e^2 H_0^{-1}$ . This allows one to model the signal expected from the two effects for an assumed  $H_0$  and check its agreement with the observations of the X-ray brightness and the SZ signal strength.

One needs to be careful, however, about the assumptions done for the analysis. Let us discuss two of them.

*ICM profile model.* The models used for the electron number density distribution and the electron pressure distribution in the cluster could introduce biases in the final result. Bonamente et al. [14] have shown, however, that the results of the calculation do not depend strongly on the models used. In their analysis the two estimates derived using two different models resulted to be in agreement.

*Deviations of cluster shape from spherical.* A large uncertainty in the calculation of the Hubble parameter could be introduced by assuming the sphericity of the cluster. Deviations from spherical shape will result in underestimation or overestimation of the Hubble constant. In short this can be written through the following ratio:

$$f_H = \frac{H_{est}}{H_{real}} = \frac{r_{\perp}}{r_{\parallel}}, \quad (9)$$

where  $r_{\perp}$  is the radius that the cluster is assumed to have (hence its extent in the plane of the sky) and  $r_{\parallel}$  is its extent in the direction of the line of sight (LOS).

So by assuming the cluster to be spherical, we will be underestimating the Hubble constant in the case when  $r_{\parallel} > r_{\perp}$  (cluster prolate in the direction of the LOS). Instead when  $r_{\parallel} < r_{\perp}$  (cluster oblate in the direction of the LOS) the Hubble constant will be overestimated. According to Sulkanen et al. [15] inclusion of a large number of clusters in the analysis allows to diminish the bias introduced by the asphericity of the individual clusters. This however will not be true if the sample used is predominantly prolate or oblate along our line of sight. There could be an intrinsic bias in the cluster sample, for example, if we happened to be more likely to detect clusters that are prolate in the LOS since the signal from such clusters would be stronger.

This means that there is a need to find a way to quantify the predominance of one or the other type of clusters in the sample. According to Kawhara et al. [16] the distribution of the measured individual  $H_{est}$  values for a set of clusters can give us hints about any biases inside the sample. Predominantly prolate samples will lead to a negatively skewed distribution and predominantly oblate samples to a positively skewed distribution.

We try to do a similar investigation by theoretically simulating clusters as triaxial ellipsoids with randomly distributed axis ratios in the range from 0.65 to 1 as is done in Sulkanen et al. We then give them random orientations in the sky calculating analytically the ratio  $f_H$  from Eq. 9. We find that the claim of Kawhara et al. is true only for axisymmetric clusters (clusters with two equal axes and fixed axis ratios), which is the type of clusters Kawhara et al. investigate. They simulate a single axisymmetric ellipsoid with fixed axis ratios (0.5 : 0.5 : 1 or 0.5 : 1 : 1) and orient it randomly in the sky. The result is illustrated on the right side of Fig. 2.

On the contrary, the shape of the distribution does not change as obviously for the case of 10000 triaxial ellipsoids, where all three axis sizes are assigned randomly. On the left part of Fig. 2 we show the resultant distributions for our theoretical simulation of a set of triaxial ellipsoidal clusters with random orientations in the sky. Hence the distribution of  $f_H$  for a set of

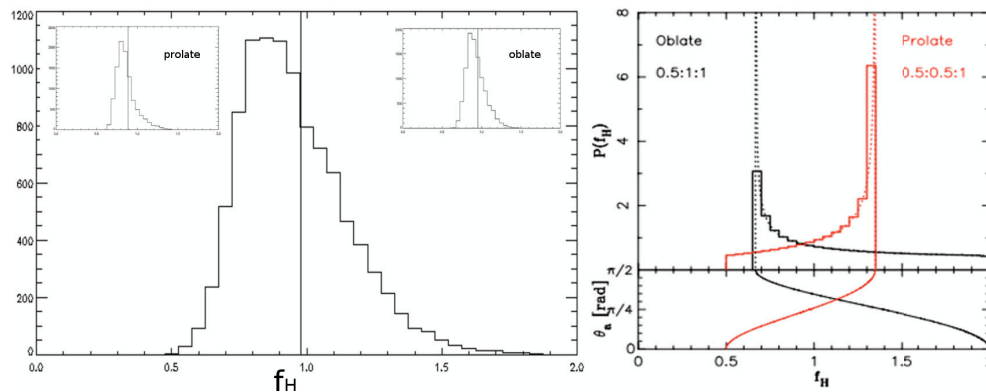


**Figure 2.** Distribution of the ratio between estimated and real value of the Hubble constant. On the left we show the changes in the distribution when predominantly prolate or oblate clusters are used. In this case different clusters with random axis ratios were simulated. The vertical solid line shows the average of each distribution. On the right we show the figure from [16] where axisymmetric clusters were used with a fixed axis ratio. In this case the distribution was derived by randomly orienting a single cluster with respect to the line of sight.

triaxial clusters in the sky will not always result in an obviously skewed distribution. We conclude that the skewness of the distribution is not a robust quantity. Some other characteristic of the distribution needs to be found in order to trace any cluster geometry biases in the experimental sample. A more refined analysis of those distributions is necessary with both theoretically created samples and clusters from simulations.

#### 4. Conclusions

We have described a method to derive the Hubble constant from joint X-ray and SZ measurements of galaxy clusters. This could provide an additional insight into the discordance of the estimates of the Hubble constant from the CMB and local tracers. We have additionally investigated the possible bias introduced by the geometry of the clusters and the possibility to identify this bias from characteristics of the distribution of estimates of  $H_0$ . We have demonstrated that it is not a straightforward task as it was suggested in [16] and a further investigation is required.

#### References

- [1] Ade P A R *et al.* (Planck Collaboration) 2016 *A&A* **596**
- [2] Riess A G *et al.* 2016 *ApJ* **826**
- [3] Cheng C *et al.* 2015 *Sci China-Phys Mech Astron* **58**
- [4] Bennett C L *et al.* 2014 *ApJ* **794**
- [5] Bonamente M *et al.* 2013 *Proc. Int. Astronomical Union, IAU Symposium* **289** 339–343
- [6] Sarazin C L 1988 *X-ray emission from clusters of galaxies* (Cambridge/New York/New Rochelle/Melbourne/Sydney: Cambridge University Press)
- [7] Sunyaev R A and Zeldovich Y B 1970 *Astrophysics and Space Science* **7** 3–19
- [8] Carlstrom J E *et al.* 2002 *Ann.Rev.A&A* **40** 643–680
- [9] Rephaeli Y *et al.* 1995 *ApJ* **445** 33–36
- [10] Aghanim N *et al.* 2009 *A&A* **496** 637–644
- [11] Adam R *et al.* (Planck Collaboration) 2016 *A&A* **594**
- [12] Adam R *et al.* (Planck Collaboration) 2016 *A&A* **594**
- [13] Meisner A *et al.* 2014 *ApJ* **798**
- [14] Bonamente M *et al.* 2006 *ApJ* **647**
- [15] Sulkanen M E *et al.* 2006 *ApJ* **522** 917–936
- [16] Kawahara H *et al.* 2008 *ApJ* **674**